

EFFECT OF TEMPERATURE ON ADAPTIVE EVOLUTION OF PHYTOPLANKTON CELL SIZE*

Ming Chen¹, Meng Fan^{2,†} and Xin Wang³

Abstract We present a simple nutrient–phytoplankton model that incorporates adaptive evolution and allometric relations. This model allows us to examine the patterns and consequences of adaptive changes in the cell size of phytoplankton under the effect of changes in water temperature. A theoretical study reveals that the ecological reproductive index can be used to characterize the evolutionary dynamics of the nutrient–phytoplankton model. Numerical analysis suggests that phytoplankton should evolve toward the small sizes typical of picophytoplankton as the water temperature increases. This study provides a framework for studying the adaptive evolution of phytoplankton cell size in water ecosystem.

Keywords Adaptive evolution, phytoplankton, body size, ecological reproductive index, temperature.

MSC(2010) 34D20, 92B05, 92D25.

1. Introduction

Phytoplankton is a polyphyletic group of single-celled primary producers that are ubiquitous in aquatic ecosystems. A diverse phytoplankton assemblage composed of species of different sizes, has existed for hundreds of millions of years, the result of long-term evolution [16]. The cell size of phytoplankton ranges over several different orders of magnitude. Body size is one of the most fundamental traits of organisms, affecting almost all aspects of their physiology and ecology. Phytoplankton cell size affects not only physiological rates but also community structure and ecological function [11, 23]. Thus, it is thought to be a promising ecophysiological trait for modeling and tracking population dynamics in response to biotic and abiotic factors [16].

Water temperature is a key environmental factor for the aquatic ecosystem, and has essential impacts on the nutrient uptake, growth, and death of phytoplankton. Therefore, water temperature can alter the productivity and composition of phytoplankton communities, thereby affecting global biogeochemical cycles [21, 28, 29].

[†]The corresponding author. Email address:mfan@nenu.edu.cn(M. Fan)

¹School of Science, Dalian Maritime University, Dalian 116026, China

²School of Mathematics and Statistics, Northeast Normal University, Changchun 130024, China

³College of Mathematics and Information Science, Anshan Normal University, Anshan 114016, China

*The authors were supported by the National Natural Science Foundation of China (No. 11671072, 12071068, 11801052) and the Natural Science Foundation of Liaoning Province (No. 2019-ZD-1056, 20180550754).

Recent studies [22] show that temperature alone is able to explain 73% of the variance in the relative contribution of small cells to total phytoplankton biomass, regardless of differences in trophic status or inorganic nutrient loading. There also exists an interesting phenomenon whereby small phytoplankton species dominate the equatorial and subtropical oceans while larger species are more abundant in subpolar regions [30]. This phenomenon is the result of long-term evolution related to water temperature. This evidence demonstrates that water temperature plays an important role in phytoplankton evolution. Hence, it is important and reasonable to incorporate all possible direct temperature effects on phytoplankton evolution into any mathematical modeling approach. Nevertheless, most mathematical modeling studies on the evolution of phytoplankton have ignored the impact of water temperature [15, 16]. Continued and increasing global warming raises two interesting questions: how do the phytoplankton communities respond to global warming, and how does the cell size of phytoplankton evolve under the impact of global warming over the long term?

There have been many conceptual, experimental, and theoretical attempts to predict the evolution of phytoplankton cell size [2, 14, 15, 19]. Adaptive dynamics provide a useful framework for modeling the evolution of quantitative traits. This approach assumes that evolutionary and ecological dynamics occur on different time-scales, separates the two dynamical processes analytically, and draws on the feedback between ecological and evolutionary processes [12, 15]. In the adaptive dynamics approach to modeling evolutionary changes in dynamical models of ecological communities, the evolutionary processes are usually governed by two important indexes, i.e., invasion fitness and fitness gradient. Species always evolve to maximize their fecundity in a specific environment. In [5], an ecological reproductive index is defined to measure the fecundity and characterize the growth of phytoplankton, which also allows a comprehensive analysis of the role of temperature on phytoplankton's growth and reproductive characteristics. This suggests another question to be addressed: what role does the ecological reproductive index play in the adaptive dynamics of phytoplankton?

Motivated by the above considerations, the principal aims of this study are twofold. The first is to develop a new reproductive index that characterizes the evolutionary dynamics of phytoplankton cell size. The second is to explore the patterns and consequences of the evolutionary trait (i.e., cell size) and investigate the impacts of water temperature on the evolutionary dynamics. In Section 2, we establish a nutrient–phytoplankton model that consider the effect of water temperature on the adaptive evolution of phytoplankton cell size, and then explore the global dynamics of the model with the help of a newly defined ecological reproductive index, R_0 . Section 3 formulates an evolutionary model and theoretically studies the evolutionary behavior of phytoplankton cell size with the help of R_0 and pairwise invisibility plots. Section 4 is devoted to investigating the effects of water temperature on the evolution dynamics of phytoplankton. Finally, Section 5 ends this paper with a discussion of the main results.

2. Ecological model

In this section, we focus on the dynamical ecological interaction between the phytoplankton and the nutrient (say phosphorus). Phytoplankton cells take a wide variety of different forms, including filamentous shapes and the presence of spines. Without

any loss of generality, the volume of differently shaped cells (V_{cell}) can be converted into the estimated spherical diameter (ESD) via the equation $ESD=2(3V_{cell}/4\pi)^{1/3}$ [24]. To facilitate the following discussion, we use the ESD defined in [24] and applied in [16] to represent the phytoplankton cell size.

2.1. Model formulation

Let $N(t)$ be the density of soluble mineral nutrient in units of milligrams of nutrient per stere and let $P(t)$ be the density of phytoplankton at time t in units of cell number per stere. The dynamical interaction between the limiting nutrient and the phytoplankton is described by

$$\begin{aligned}\frac{dN}{dt} &= D(N_{in} - N) - Q(x)\mu_{opt}(x)h(T)f(N)P, \\ \frac{dP}{dt} &= \mu_{opt}(x)h(T)f(N)P - mP - s(x)k(T)P,\end{aligned}\tag{2.1}$$

where $D(N_{in} - N)$ models the nutrient exchange with an external source; $\mu_{opt}(x)$ is the maximum specific growth rate (day^{-1}) of phytoplankton, $s(x)$ is the loss rate (day^{-1}), $Q(x)$ is the amount of nutrient in an individual cell ($\text{mg} \cdot \text{cell}^{-1}$), which are all size dependent (i.e., function of ESD x); m is the specific mortality rate (day^{-1}) of phytoplankton, which is size-independent; $f(N)$ represents the nutrient limitation experienced by phytoplankton; $h(T)$ and $k(T)$ represent the temperature limitations on the growth rate and loss rate of phytoplankton, respectively.

In (2.1), the comprehensive impact of the cell size and water temperature on the growth and loss of phytoplankton is assumed to be of multiplicative type. The maximum specific growth rate of phytoplankton, $\mu_{opt}(x)$, does not bear a simple relationship with size over the possible range of phytoplankton cells [16]. Many factors related to cell size impact the loss rate $s(x)$ of phytoplankton, as do the natural mortality, sinking, intraspecific competition, and predation by higher trophic levels (such as zooplankton and fish) [31, 32]. Therefore, in different cases, $\mu_{opt}(x)$ and $s(x)$ can take different forms.

To characterize the effect of temperature on the adaptive evolution of phytoplankton, we first define an ecological reproductive index of phytoplankton as

$$R_0 = \frac{\mu_{opt}(x)h(T)f(N_{in})}{m + s(x)k(T)},\tag{2.2}$$

which is a function of cell size x . R_0 is a key indicator of phytoplankton fecundity, measuring the average newborn phytoplankton produced by one unit of phytoplankton during the phytoplankton life span [5].

2.2. Global dynamics

In this study, we assume that $f(N)$ in system (2.1) is a bounded and smooth function satisfying [20]

$$f(0) = 0, \quad f'(N) > 0, \quad f'(0) < \infty \quad \text{and} \quad f''(N) < 0 \quad \text{for} \quad N > 0.$$

Theorem 2.1. *If $R_0 > 1$, then (2.1) has a unique positive equilibrium $E^*(N^*, P^*)$ and is globally asymptotically stable.*

Proof. For the positive equilibrium $E^*(N^*, P^*)$, N^* and P^* can be determined from the following system of algebraic equations

$$\begin{aligned} D(N_{in} - N) - Q(x)\mu_{opt}(x)h(T)f(N)P &= 0, \\ \mu_{opt}(x)h(T)f(N) - m - s(x)k(T) &= 0. \end{aligned} \quad (2.3)$$

Then, by (2.3), it is easy to show that, if $R_0 > 1$,

$$N^*(x) = f^{-1}\left(\frac{m + s(x)k(T)}{\mu_{opt}(x)h(T)}\right) > 0, \quad P^*(x) = \frac{D(N_{in} - N^*(x))}{(m + s(x)k(T))Q(x)} > 0, \quad (2.4)$$

where the ecological equilibrium $E^*(N^*(x), P^*(x))$ is determined by the cell size x and temperature T . Because $f'(N) > 0$, such an $N^*(x)$ is unique. Thus, there is a unique positive equilibrium $E^*(N^*(x), P^*(x))$ of (2.1).

Consider the Lyapunov function defined by

$$V(N, P) = \int_{N^*}^N q(\xi)d\xi + \int_{P^*}^P \frac{\xi - P^*}{\xi} d\xi,$$

where

$$\begin{aligned} q(N) &:= \frac{P^*(\mu_{opt}(x)h(T)f(N) - m - s(x)k(T))}{D(N_{in} - N)} \\ &= \frac{(N_{in} - N^*)(\mu_{opt}(x)h(T)f(N) - m - s(x)k(T))}{(N_{in} - N)(m + s(x)k(T))Q(x)}. \end{aligned}$$

Differentiating $V(N, P)$ along the solutions of (2.1) and using (2.3), we obtain

$$\begin{aligned} \frac{dV}{dt} &= q(N)\frac{dN}{dt} + \frac{P - P^*}{P} \frac{dP}{dt} \\ &= q(N)[D(N_{in} - N) - Q(x)\mu_{opt}(x)h(T)f(N)P] \\ &\quad + (P - P^*)[\mu_{opt}(x)h(T)f(N) - m - s(x)k(T)] \\ &= [q(N)D(N_{in} - N) - P^*(\mu_{opt}(x)h(T)f(N) - m - s(x)k(T))] \\ &\quad + P[(\mu_{opt}(x)h(T)f(N) - m - s(x)k(T)) - q(N)Q(x)\mu_{opt}(x)h(T)f(N)] \\ &= P \cdot (\mu_{opt}(x)h(T)f(N) - m - s(x)k(T)) \cdot \left(1 - \frac{\mu_{opt}(x)h(T)f(N)(N_{in} - N^*)}{(m + s(x)k(T))(N_{in} - N)}\right) \\ &\leq 0. \end{aligned}$$

Obviously, $dV/dt = 0$ if and only if $(N, P) = (N^*, P^*)$. This implies that, when $R_0 > 1$, the largest compact invariant set of model (2.1) in $\{(N, P) \mid dV/dt = 0\}$ is the singleton $\{(N^*, P^*)\}$. By LaSalle's invariant principle [18], $E^*(N^*, P^*)$ is globally asymptotically stable when $R_0 > 1$. \square

3. Evolutionary model

In this section, we establish a resident–mutant model to explore the effect of temperature on the adaptive evolution of phytoplankton. Consider the body or cell size as the evolutionary trait of phytoplankton, and assume that the rate of change of this trait is slower than the ecological dynamics.

3.1. Model formulation

When a mutant phytoplankton population with a slightly different cell size y appears, it is reasonable and realistic to ask which population will become dominant in the system. To derive the invasion fitness for mutant phytoplankton and model the dynamics of the resident-mutant population, we modify the resident phytoplankton model (2.1) to

$$\begin{aligned}\frac{dN}{dt} &= D(N_{in} - N) - \mu_{opt}(x)h(T)f(N)PQ(x) - \mu_{opt}(y)h(T)f(N)P_mQ(y), \\ \frac{dP}{dt} &= \mu_{opt}(x)h(T)f(N)P - mP - s(x)k(T)P, \\ \frac{dP_m}{dt} &= \mu_{opt}(y)h(T)f(N)P_m - mP_m - s(y)k(T)P_m,\end{aligned}\tag{3.1}$$

where P_m denotes the population density of mutant phytoplankton. Before the occurrence of the mutation, the resident population density is stable at $(N^*(x), P^*(x))$ under system (2.1). Just after the occurrence of a rare mutation, however, the resident and mutant populations are close to the ecological equilibrium $(N^*(x), P^*(x), 0)$ of (3.1). That is, the stability of $(N^*(x), P^*(x), 0)$ is crucial in determining whether the mutant phytoplankton can invade. The stability of this ecological equilibrium is now analyzed.

The Jacobian matrix of (3.1) at $(N^*(x), P^*(x), 0)$ takes the form

$$J(N^*(x), P^*(x), 0) = \begin{pmatrix} J_{sub} & J_0 \\ \mathbf{0} & \mu_{opt}(y)h(T)f(N^*(x)) - m - s(y)k(T) \end{pmatrix},$$

where

$$J_{sub} = \begin{pmatrix} -D - Q(x)\mu_{opt}(x)h(T)f'(N^*(x))P^*(x) & -\mu_{opt}(x)h(T)f(N^*(x))Q(x) \\ \mu_{opt}(x)h(T)f'(N^*(x))P^*(x) & \mu_{opt}(x)h(T)f(N^*(x)) - m - s(x)k(T) \end{pmatrix}$$

and

$$J_0 = \begin{pmatrix} -\mu_{opt}(y)h(T)f(N^*(x))Q(y) \\ 0 \end{pmatrix}.$$

Note that J_{sub} is the Jacobian matrix of model (2.1) at $E^*(N^*(x), P^*(x))$. All the eigenvalues of J_{sub} have negative real parts when $R_0 > 1$.

Note that the third eigenvalue of $J(N^*(x), P^*(x), 0)$ is

$$\mu_{opt}(y)h(T)f(N^*(x)) - m - s(y)k(T),\tag{3.2}$$

which denotes the per capita growth rate of a very scarce mutant phytoplankton with cell size y . To facilitate the following discussion, we define this quantity as $F(y, x)$. If $F(y, x) < 0$, then $(N^*(x), P^*(x), 0)$ is asymptotically stable, which means that the mutant phytoplankton population fails to invade and tends to become extinct; if $F(y, x) > 0$, then $(N^*(x), P^*(x), 0)$ is unstable, which means that the abundance of the mutant phytoplankton will initially increase, that is, the mutant phytoplankton population can invade. Because of its important role in determining the fate of the mutant phytoplankton, $F(y, x)$ is called the invasion eigenvalue

or invasion fitness. This measures the initial exponential growth rate of the mutant phytoplankton population in an environmental set dominated by the resident population [33].

If the mutants are rare and have a relatively small effect, then the cell size of the phytoplankton will evolve through both successive invasions and replacements along the direction predicted by the sign of the local selection gradient $g(x)$, which can be obtained by taking the derivative of $F(y, x)$ with respect to the mutant cell size y and evaluating it at the resident phytoplankton cell size x [33]. Then,

$$g(x) = \frac{\partial F(y, x)}{\partial y} \Big|_{y=x} = \mu'_{opt}(x)h(T)f(N^*(x)) - s'(x)k(T). \quad (3.3)$$

The continuity of the selection gradient $g(x)$ with respect to x and the small difference between cell sizes x and y in the early stage of mutation mean that the mutant's fitness can be linearly approximated by

$$F(y, x) = g(x)(y - x). \quad (3.4)$$

According to (3.4), a positive selection gradient $g(x)$ allows the invasion of mutant phytoplankton with bigger cell sizes, whereas a negative $g(x)$ is conducive to the successful invasion of mutant phytoplankton with smaller cell sizes.

When mutants with higher fitness values appear, evolution occurs. Following the results of [1, 9], if the mutation processes are homogeneous and the mutations are rare and have a relatively small effect, it can be assumed that the rate of change in the mean cell size of the phytoplankton will be proportional to the fitness gradient $g(x)$, i.e.,

$$\frac{dx}{dt} = \frac{1}{2}r\sigma^2 P^*(x)g(x), \quad (3.5)$$

where r is the birth probability of mutant phytoplankton, σ^2 is the variance of the mutation distribution, and $P^*(x)$ is the equilibrium population density of phytoplankton satisfying (2.3). The factor $(1/2)r\sigma^2$ is called the mutation rate. Together with the population density $P^*(x)$, this determines the rate of evolutionary change [8]. Equation (3.5) governs the variation of the cell size.

3.2. Evolutionary analysis

One of the central issues of evolutionary dynamics is to characterize the evolutionary process at community levels, such as whether it is a continuously stable strategy, an evolutionary repeller, or some other process.

Definition 3.1 ([12]). A trait x^* is said to be an evolutionarily singular strategy if the selection gradient (3.3) vanishes at x^* .

According to Definition 3.1, the evolutionarily singular strategy x^* satisfies $g(x^*) = 0$. In addition to the invasion fitness (3.2) and fitness gradient (3.3), we now study the evolutionarily singular strategy in terms of the basic reproductive index defined in (2.2).

Theorem 3.1. *The evolutionarily singular strategy x^* of system (3.5) occurs when $\frac{\partial R_0}{\partial x} \Big|_{x=x^*} = 0$.*

Proof. The evolutionarily singular strategy x^* occurs when $g(x^*) = 0$. From (2.3), it follows that

$$\mu_{opt}(x^*)h(T)f(N^*(x^*)) = m + s(x^*)k(T).$$

A direct calculation then leads to

$$\begin{aligned} \frac{\partial R_0}{\partial x} \Big|_{x=x^*} &= \frac{\mu'_{opt}(x^*)h(T)f(N_{in})[m + s(x^*)k(T)] - s'(x^*)k(T)\mu_{opt}(x^*)h(T)f(N_{in})}{(m + s(x^*)k(T))^2} \\ &= \frac{[\mu'_{opt}(x^*)h(T)f(N^*(x^*)) - s'(x^*)k(T)] \cdot \mu_{opt}(x^*)h(T)f(N_{in})}{(m + s(x^*)k(T))^2} \\ &= \frac{g(x^*) \cdot \mu_{opt}(x^*)h(T)f(N_{in})}{(m + s(x^*)k(T))^2} = 0. \end{aligned}$$

This completes the proof. \square

Theorem 3.1 tells us that the evolutionarily singular strategy x^* appears at the extreme point of the function $R_0(x)$.

Definition 3.2 ([33]). An evolutionarily singular strategy x^* is said to be convergence stable if the repeated invasion of nearby mutant strategies into nearby resident strategies will lead to the convergence of resident strategies x^* .

The condition for convergence stability is given by [10, 12, 13]

$$\frac{dg(x)}{dx} \Big|_{x=x^*} < 0,$$

where $g(x)$ is the selection gradient defined by (3.3).

Definition 3.3 ([33]). An evolutionarily singular strategy x^* is said to be evolutionary stable if x^* is a maximum fitness point with respect to the mutant trait value y .

The evolutionarily singular strategy x^* is stable against the invasion of neighboring strategies. We consider the second derivative of the invasion fitness with respect to the mutant trait value y , and evaluate it at the singular point x^* . The condition for evolutionary stability is then given by [7, 12, 27]

$$\frac{\partial^2 F(y, x)}{\partial y^2} \Big|_{y=x^*} < 0.$$

Definition 3.4 ([33]). An evolutionarily singular strategy x^* is said to be a continuously stable strategy if x^* is both evolutionary stable and convergence stable.

Definition 3.5 ([12]). An evolutionarily singular strategy x^* is said to be an evolutionary repeller if x^* is neither convergence stable nor evolutionary stable.

Convergence stability and evolutionary stability identify the dynamical behavior of evolutionarily singular strategy x^* . We next analyze the convergence stability and evolutionary stability of the evolutionarily singular strategy x^* with the help of the ecological reproductive index.

Theorem 3.2. *Let x^* be an evolutionarily singular strategy of (3.5).*

- *If $\frac{\partial^2 R_0}{\partial x^2}|_{x=x^*} < 0$, then x^* is a continuously stable strategy.*
- *If $\frac{\partial^2 R_0}{\partial x^2}|_{x=x^*} > 0$, then x^* is an evolutionary repeller.*

Proof. For system (3.5), we have

$$\frac{\partial^2 F(y, x)}{\partial y^2} \Big|_{y=x=x^*} = \mu''_{opt}(x^*)h(T)f(N^*(x^*)) - s''(x^*)k(T). \quad (3.6)$$

Note that

$$\begin{aligned} \mu_{opt}(x^*)h(T)f(N^*(x^*)) - m - s(x^*)k(T) &= 0, \\ \mu'_{opt}(x^*)h(T)f(N^*(x^*)) - s'(x^*)k(T) &= 0. \end{aligned} \quad (3.7)$$

From (2.4) and (3.7), it follows that

$$\begin{aligned} & \frac{\partial f(N^*)}{\partial x} \Big|_{x=x^*} \\ &= \frac{s'(x^*)k(T) \cdot \mu_{opt}(x^*)h(T) - (m + s(x^*)k(T)) \cdot \mu'_{opt}(x^*)h(T)}{(\mu_{opt}(x^*)h(T))^2} \\ &= \frac{\mu'_{opt}(x^*)h(T)f(N^*(x^*)) \cdot \mu_{opt}(x^*)h(T) - \mu_{opt}(x^*)h(T)f(N^*(x^*)) \cdot \mu'_{opt}(x^*)h(T)}{(\mu_{opt}(x^*)h(T))^2} \\ &= 0. \end{aligned} \quad (3.8)$$

Then

$$\begin{aligned} \frac{dg(x)}{dx} \Big|_{x=x^*} &= \mu''_{opt}(x^*)h(T)f(N^*(x^*)) + \mu'_{opt}(x^*)h(T) \frac{\partial f(N^*)}{\partial x} \Big|_{x=x^*} - s''(x^*)k(T) \\ &= \mu''_{opt}(x^*)h(T)f(N^*(x^*)) - s''(x^*)k(T). \end{aligned} \quad (3.9)$$

From (3.8), we have

$$\frac{\partial^2 R_0}{\partial x^2} \Big|_{x=x^*} = \frac{[\mu''_{opt}(x^*)h(T)f(N^*(x^*)) - s''(x^*)k(T)]\mu_{opt}(x^*)h(T)f(N_{in})}{(m + s(x)k(T))^2}. \quad (3.10)$$

By (3.6), (3.9) and (3.10), if $\partial^2 R_0/\partial x^2|_{x=x^*} < 0$, then

$$\frac{\partial^2 F(y, x)}{\partial y^2} \Big|_{y=x=x^*} < 0, \quad \frac{dg(x)}{dx} \Big|_{x=x^*} < 0,$$

and so x^* is a continuously stable strategy. If $\partial^2 R_0/\partial x^2|_{x=x^*} > 0$, then

$$\frac{\partial^2 F(y, x)}{\partial y^2} \Big|_{y=x=x^*} > 0, \quad \frac{dg(x)}{dx} \Big|_{x=x^*} > 0,$$

and x^* is an evolutionary repeller. \square

In general, for the given trade-off functions, on the curve defined by the ecological reproductive index with respect to the cell size, the evolutionarily singular points

x^* of system (3.5) at the local “peaks” of the curve denote the continuously stable strategies. The evolutionarily singular points x^* of system (3.5) at the local “valleys” of the curve denote the evolutionary repellers. Theorems 3.1 and 3.2 reveal that the phytoplankton cell size will always evolve to maximize its fecundity for the current environment.

The evolutionary dynamics of system (3.5), characterized by Theorems 3.1 and 3.2, can be intuitively represented with the help of the basic reproductive index and pairwise invisibility plots. Figure 1 illustrates such a scenario, where the parameter values and trade-off functions are deliberately specified such that the curve defined by $R_0(x)$ admits both “peaks” and “valleys”. In Figure 1-(a), Theorem 3.1 implies that the two solid points and one hollow point satisfy $\partial R_0/\partial x|_{x=x^*} = 0$, and thus denote evolutionarily singular strategies. By Theorem 3.2, the two solid points at the local “peaks” of the curve satisfying $\partial^2 R_0/\partial x^2|_{x=x^*} < 0$ are continuously stable strategies, whereas the hollow point at the local “valley” of the curve satisfying $\partial^2 R_0/\partial x^2|_{x=x^*} > 0$ is an evolutionary repeller. The pairwise invisibility plot (Fig. 1-(b)) shows that, in the dark (+) region, the mutants have positive fitness values, which implies that the mutant population can invade; in the white (−) region, the mutant have negative fitness, which means the mutant population can not survive. In particular, in the dark (+) region on the left side of the vertical line through x_2^* , x_1^* is convergence stable and the local fitness gradient points toward the singular strategy x_1^* ; in the dark (+) region on the right side of the vertical line through x_2^* , x_3^* is convergence stable and the local fitness gradient points toward the singular strategy x_3^* .

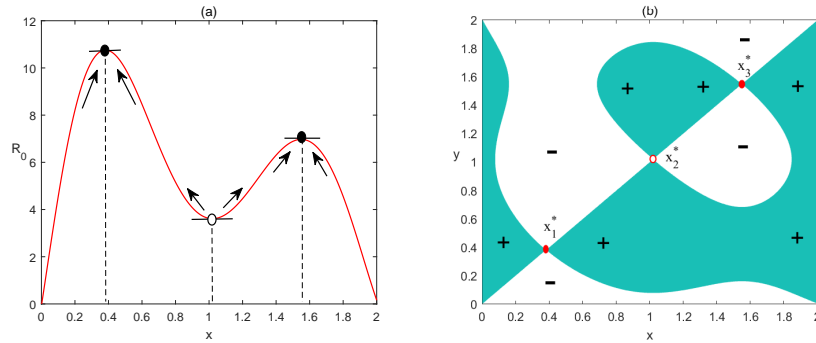


Figure 1. (a) Plot of basic reproductive index with respect to cell size (x), where the solid points at the “peaks” represent the continuously stable strategies, the hollow point at the “valley” represents the evolutionary repeller, and the arrows denote the directions as x evolves. (b) Pairwise invisibility plot, where the dark region with ‘+’ corresponds to resident–mutant pairs (x, y) that allow the mutant to invade (i.e., $F(y, x) > 0$) and the white region with ‘−’ denotes the region in which the mutant can not invade (i.e., $F(y, x) < 0$).

4. Impact of temperature on evolution of cell size

In this section, we analytically investigate how the evolutionary model responds to variations in water temperature.

Theorem 4.1. *Assume that*

$$k'(T) \cdot [\mu''_{opt}(x^*)s'(x^*) - \mu'_{opt}(x^*)s''(x^*)] < 0. \tag{4.1}$$

Then, the evolutionarily singular point x^* of (3.5) is decreasing with respect to water temperature T .

Proof. From Theorem 3.1 and (3.3), it follows that

$$\mu'_{opt}(x^*)h(T)f(N^*(x^*)) - s'(x^*)k(T) = 0. \quad (4.2)$$

By (2.4), we have

$$\mu'_{opt}(x^*)h(T) \cdot \frac{m + s(x^*)k(T)}{\mu_{opt}(x^*)h(T)} - s'(x^*)k(T) = 0.$$

Then,

$$k(T) = \frac{m\mu'_{opt}(x^*)}{\mu_{opt}(x^*)s'(x^*) - \mu'_{opt}(x^*)s(x^*)} := H(x^*), \quad (4.3)$$

which implies that the effect of temperature on the evolutionarily singular point x^* is related to the temperature-dependent loss rate. A direct calculation produces

$$H'(x^*) = \frac{m[\mu''_{opt}(x^*)s'(x^*) - \mu'_{opt}(x^*)s''(x^*)]}{[\mu_{opt}(x^*)s'(x^*) - \mu'_{opt}(x^*)s(x^*)]^2}.$$

Hence, (4.1) implies that $k(T)$ and $H(x^*)$ have opposite monotonic trends. Equation (4.3) indicates that x^* is decreasing with respect to T when (4.1) holds. \square

We next discuss the biological significance of (4.1). It is assumed that phytoplankton cells are spherical. Therefore, the loss rate of a cell with a ESD of x increases in proportion to the square of its diameter [16, 17]. This fact implies that $s'(x^*) > 0$ and $s''(x^*) < 0$. For species with a relatively large cell size, as the cell size increases, the maximum specific growth rate tends to decline with a decelerating rate [16], presumably because it is more efficient for smaller cells to acquire resources [25]. An examination of picophytoplankton shows that the maximum specific growth rate tends to increase with size, mainly for the limited supply of cellular catalysts in extremely small cells [25]. These patterns require $\mu_{opt}(x)$ to satisfy $\mu'_{opt}(x) > 0$ and $\mu''_{opt}(x) < 0$ for small x , and $\mu'_{opt}(x) < 0$ and $\mu''_{opt}(x) > 0$ for relatively large x . Equation (4.2) together with positive $s'(x^*)$ results in

$$\mu'_{opt}(x^*) = \frac{h(T)f(N^*(x^*))}{s'(x^*)k(T)} > 0,$$

which implies that the evolutionarily singular point x^* should fall in the range where $\mu'_{opt}(x^*) > 0$ and $\mu''_{opt}(x^*) < 0$. The monotonicity of $s(x^*)$ and $\mu_{opt}(x^*)$ leads to

$$H'(x^*) < 0. \quad (4.4)$$

The loss rate is temperature-dependent and various candidates have been suggested to account for this dependence [17]. The temperature-dependent loss rate $k(T)$ is chosen to be a monotonic increasing function [17]. Then we have

$$k'(T) > 0. \quad (4.5)$$

Equations (4.4) and (4.5), deduced by empirical patterns, ensure that (4.1) holds.

To clarify the effect of temperature on the evolution of phytoplankton cell size, (2.1) should be specified using some empirical models. Table 1 illustrates some typical examples of the functions in (2.1) satisfying (4.1) of Theorem 4.1. In Table 1, the effect of temperature on the growth of phytoplankton is described by the so-called cardinal temperature model with inflexion (CTMI) [26], which has been validated for a large range of phytoplankton species [6]. In addition, the nutrient quota of a cell is assumed to be directly proportional to its volume, i.e., the cube of its ESD [16]. The parameter values are listed in Table 2.

Table 1. Empirical models for system (2.1) used for numerical studies

| Func. | Description | Concrete form | Ref. |
|----------------|--|---|------|
| $Q(x)$ | cell size dependent nutrient quota of a cell | $Q(x) = \beta x^3$ | [16] |
| $\mu_{opt}(x)$ | cell size dependent growth rate | $\mu_{opt}(x) = \frac{x}{a_1 x^2 + a_2 x + a_3}$ | [16] |
| $s(x)$ | cell size dependent loss rate | $s(x) = \alpha x^2$ | [16] |
| $h(T)$ | temperature dependent growth rate | $h(T) = \begin{cases} 0 & \text{for } T < T_{min}, \\ \phi(T) & \text{for } T_{min} < T < T_{max}, \\ 0 & \text{for } T > T_{max}, \end{cases}$ | [3] |
| $k(T)$ | temperature dependent loss rate | $k(T) = \sqrt{\frac{T}{T_{ref}}}$ | [17] |
| $f(N)$ | functional response | $f(N) = \frac{N}{H + N}$ | [4] |

Notes: $\phi(T) = \frac{(T - T_{max})(T - T_{min})^2}{(T_{opt} - T_{min})[(T_{opt} - T_{min})(T - T_{opt}) - (T_{opt} - T_{max})(T_{opt} + T_{min} - 2T)]}$.

Table 2. Parameters of system (2.1) with default values used for numerical studies

| Par. | Description | Value | Unit | Ref. |
|-----------|---|-------|--|-----------|
| T_{opt} | optimal water temperature | 20 | °C | [3] |
| T_{min} | minimum water temperature | -5 | °C | [3] |
| T_{max} | maximum water temperature | 30 | °C | [3] |
| T_{ref} | reference water temperature | 25 | °C | [17] |
| α | constant affected by the density of the water | 0.1 | $(\mu\text{m})^{-2} \cdot \text{day}^{-1}$ | [16] |
| β | quota for $x = 1$ | 10 | $(\mu\text{m})^{-3}$ | [16] |
| a_1 | constant for cell size | 0.02 | $(\mu\text{m})^{-1} \cdot \text{day}$ | [16] |
| a_2 | constant for cell size | 0.02 | day | [16] |
| a_3 | constant for cell size | 0.08 | $\mu\text{m} \cdot \text{day}$ | [16] |
| m | natural mortality rate of phytoplankton | 0.15 | day^{-1} | [5] |
| H | half-saturation constant for nutrient uptake | 0.05 | $\text{mg} \cdot \text{L}^{-1}$ | [5] |
| N_{in} | density of total input soluble phosphorus | 0.5 | $\text{mg} \cdot \text{L}^{-1}$ | Defaulted |
| D | dilution rate | 0.5 | day^{-1} | Defaulted |

Figure 2 shows the results of numerical simulations of the ecological reproductive index with respect to cell size along the gradient of water temperature T , from low temperature (e.g., 4 °C) to high temperature (e.g., 28 °C). From Theorems 3.1 and 3.2, we know that the red solid points at the peaks of the curves defined by $R_0(x)$ represent the continuously stable strategies x^* at different temperatures.

Let \hat{R}_0 be the basic reproductive value at the given temperature T and the corresponding continuously stable strategy x^* , i.e., $\hat{R}_0 = R_0(T, x^*)$, which measures the evolutionarily stable fecundity of phytoplankton at different temperatures. When the water temperature is below the optimal level (e.g., 20 °C), the evolutionarily stable fecundity of phytoplankton \hat{R}_0 increases, but the cell size x^* decreases with an increase in water temperature (Fig. 2-(a)). When the water temperature is above the optimal level, both \hat{R}_0 and x^* decrease as the temperature increases (Fig. 2-(b)). Moving the temperature away from the optimal level has a negative effect on the fecundity of phytoplankton.

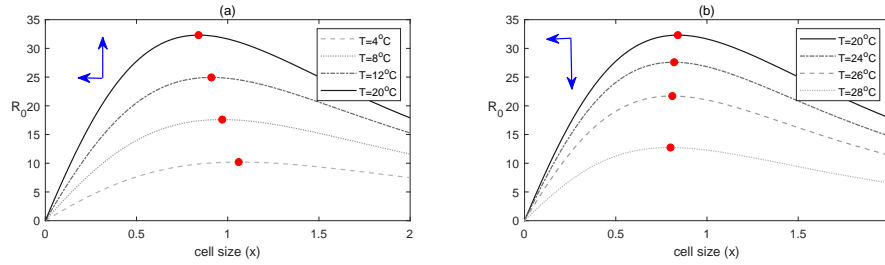


Figure 2. Basic reproductive index with respect to cell size x with varying temperature. The solid point at the local “peak” of the curve represents the continuously stable strategy. (a) Water temperature below the optimal level. (b) Water temperature above the optimal level. The horizontal arrows represent the directions as x^* evolves with increasing temperature. The vertical arrows represent the directions as the evolutionarily stable fecundity of phytoplankton \hat{R}_0 varies with increasing temperature.

Figure 3 gives a full picture of the effect of water temperature on the evolutionarily stable fecundity of phytoplankton \hat{R}_0 and evolutionarily stable phytoplankton cell size x^* . Figure 3-(a) shows that the evolutionarily stable fecundity of phytoplankton first increases and then decreases as the water temperature rises. The evolutionarily stable fecundity of phytoplankton achieves a maximum value at some optimal temperature. Figure 3-(b) elaborates the relationship between cell size and water temperature. It shows that the phytoplankton cell size decreases as the temperature rises, and is always above a positive minimum level.

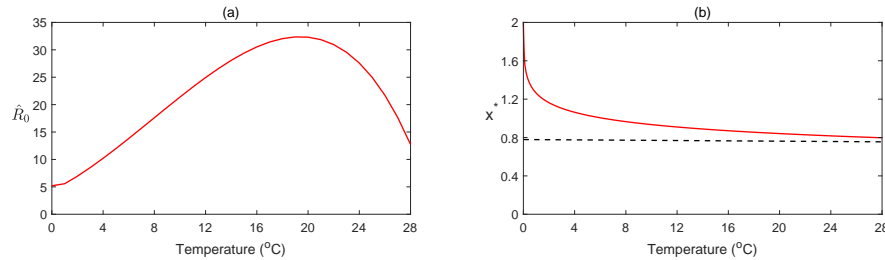


Figure 3. (a) Effect of increasing temperature on the evolutionarily stable fecundity of phytoplankton \hat{R}_0 . (b) Effect of increasing temperature on the cell size x^* under the continuously stable strategy. The dashed line denotes the minimum phytoplankton cell size.

5. Conclusions

Adaptive dynamics are an effective approach for studying the evolutionary phenotypic changes in evolving populations when the fitness is density- or frequency-

dependent [12]. This study has investigated the evolutionary dynamics of a single population of phytoplankton with varying water temperature.

A nutrient–phytoplankton model incorporating the effect of temperature and cell size was first formulated and then fully analyzed. Based on the globally asymptotically stable internal equilibrium, we proposed an evolutionary model of cell size and examined its evolutionary dynamics by investigating both the convergence stability and evolutionary stability. Equation (3.5) is much more general and flexible in terms of admitting different concrete functional forms of cell size and temperature. The criteria established to characterize the evolutionary dynamics of (3.5) (i.e., Theorem 3.1 and 3.2) are independent of the functional forms of the cell size and temperature. It is the limiting factors, not their concrete functional forms, which assert a significant impact on the phytoplankton dynamics.

The ecological reproductive index R_0 measures the fecundity of phytoplankton and plays an important role in characterizing their evolutionary dynamics. Theoretical analysis has revealed that the evolutionarily singular strategy x^* of system (3.5) occurs at the points where the derivative of R_0 is equal to zero. Moreover, the evolutionarily singular strategy x^* of (3.5) at the local “peaks” of the curve defined by $R_0(x)$ is a continuously stable strategy, and the evolutionarily singular strategy at the local “valleys” is an evolutionary repeller. Numerical simulations have been conducted to confirm the theoretical analysis.

The important insights obtained from accurate computations indicate that the continuously stable strategy is affected by the temperature dependent loss rate rather than the growth rate. To adapt to increasing temperatures, the cell size of phytoplankton evolves to decrease and maximize its fecundity, but never falls below a minimum value. The continuous stable fecundity depicted by the ecological reproductive index first increases and then decreases as the water temperature rises.

In summary, our analytical and numerical analysis suggests the following conclusions:

- In mathematical terms, unlike the traditional analysis of evolutionary dynamics using the invasion fitness and fitness gradient, this paper has proved that the ecological reproductive index is important in determining the type of singular points attained by the phytoplankton evolutionary model and characterizing the evolutionary dynamics.
- In ecological terms, it has been revealed that the evolution of the phytoplankton cell size is affected by the temperature-dependent loss rate. When the temperature increases within a reasonable range, the cell size of phytoplankton evolves to decrease. Thus, global warming will cause phytoplankton to evolve into picophytoplankton.

As phytoplankton is an assembly of organisms that arose from different evolutionary processes and present different characteristics (e.g., physiological, morphological), the extension of our evolutionary framework to include several other traits and abiotic factors should enable a more comprehensive understanding of the dynamics of aquatic ecosystems. A key challenge for future research is to investigate not only the impact of temperature on the evolution of primary producers (i.e., phytoplankton), but also the influence of comprehensive climate changes on the networks of evolutionary changes throughout the food web.

Acknowledgements

The authors are grateful to the anonymous referees for providing valuable suggestions which helped us to improve the contents of this article. We thank Stuart Jenkinson, PhD, for polishing the English text of a draft of this manuscript.

References

- [1] P. A. Abrams, M. Hiroyuki and H. Yasushi, *Evolutionarily unstable fitness maxima and stable fitness minima of continuous traits*, *Evol. Ecol.*, 1993, 7(5), 465–487.
- [2] L. T. Bach, K. T. Lohbeck, T. B. H. Reusch et al., *Rapid evolution of highly variable competitive abilities in a key phytoplankton species*, *Nat. Ecol. Evol.*, 2018, 2(4), 611.
- [3] O. Bernard and B. Remond, *Validation of a simple model accounting for light and temperature effect on microalgal growth*, *Bioresource Technol.*, 2012, 123, 520–527.
- [4] J. A. Bonachela, M. Raghieb and S. A. Levin, *Dynamic model of flexible phytoplankton nutrient uptake*, *P. Natl. Acad. Sci.*, 2011, 108, 20633–20638.
- [5] M. Chen, M. Fan, R. Liu et al., *The dynamics of temperature and light on the growth of phytoplankton*, *J. Theor. Biol.*, 2015, 385, 8–19.
- [6] M. Chen, M. Fan, X. Yuan et al., *Effect of seasonal changing temperature on the growth of phytoplankton*, *Math. Biosci. Eng.*, 2017, 289(5–6), 9–19.
- [7] F. B. Christiansen, *On conditions for evolutionary stability for a continuously varying character*, *Am. Nat.*, 1991, 1, 37–50.
- [8] U. Dieckmann, M. Paul and L. Richard, *Evolutionary cycling in predator-prey interactions: population dynamics and the Red Queen*, *J. Theor. Biol.*, 1995, 176, 91–102.
- [9] U. Dieckmann and L. Richard, *The dynamical theory of coevolution: a derivation from stochastic ecological processes*, *J. Math. Biol.*, 1996, 34(5), 579–612.
- [10] I. Eshel, *Evolutionary and continuous stability*, *J. Theor. Biol.*, 1983, 103, 99–111.
- [11] Z. V. Finkel, J. Beardall, K. J. Flynn et al., *Phytoplankton in a changing world: cell size and elemental stoichiometry*, *J. Plankton Res.*, 2010, 32(1), 119–137.
- [12] S. A. H. Geritz, G. Mesze and A. J. M. Johan, *Evolutionarily singular strategies and the adaptive growth and branching of the evolutionary tree*, *Evol. Ecol.*, 1998, 12, 35–57.
- [13] S. A. H. Geritz, K. Eva and P. Yan, *Evolutionary branching and long-term coexistence of cycling predators: critical function analysis*, *Theor. Popul. Biol.*, 2007, 71(4), 424–435.
- [14] G. M. Grimaud, L. E. Guennec, A. Valerie et al., *Modelling the effect of temperature on phytoplankton growth across the global ocean*, *Mathmod*, 2015, 48, 228–233.
- [15] L. Hao, M. Fan and X. Wang, *Effects of nutrient enrichment on coevolution of a stoichiometric producer-grazer system*, *Math. Biosci. Eng.*, 2014, 11(4), 841–875.

- [16] L. Jiang, O. M. E. Schofield and P. G. Falkowski, *Adaptive evolution of phytoplankton cell size*, *Am. Nat.*, 2005, 166(4), 496–505.
- [17] S. E. Jorgensen and B. Giuseppe, *Fundamentals of ecological modelling*, 2001.
- [18] J. P. LaSalle, *The stability of dynamical systems, regional conference series in applied mathematics*, SIAM, Pa., 1976.
- [19] E. Litchman, K. F. Edwards and C. A. Klausmeier, *Phytoplankton niches, traits and eco-evolutionary responses to global environmental change*, *Mar. Ecol. Prog. Ser.*, 2012, 470, 235–248.
- [20] I. Loladze, Y. Kuang and J.J. Elser, *Stoichiometry in producer-grazer systems: linking energy flow with element cycling*, *B. Math. Biol.*, 2000, 62(6), 1137–1162.
- [21] M. C. B. Mesquita, A. C. C. Prestes, A. M. A. Gomes et al., *Direct effects of temperature on growth of different tropical phytoplankton species*, *Microb. Ecol.*, 2019, 79(5872), 1–11.
- [22] X. A. G. Moran, N. L. P. Urrutia, C. A. Z. Alejandra et al., *Increasing importance of small phytoplankton in a warmer ocean*, *Global Change Biol.*, 2010, 16, 1137–1144.
- [23] K. H. Peter and U. Sommer, *Interactive effect of warming, nitrogen and phosphorus limitation on phytoplankton cell size*, *Ecol. Evol.*, 2015, 5(5), 1011–1024.
- [24] Z. Pu, M. H. Cortez and L. Jiang, *Predator-prey coevolution drives productivity-richness relationships in planktonic systems*, *Am. Nat.*, 2017, 189, 1–35.
- [25] J. A. Raven, *The twelfth Tansley Lecture. Small is beautiful: the picophytoplankton*, *Funct. Ecol.*, 1998, 12, 503–513.
- [26] L. Rosso, J. R. Lobry and J. P. Flandrois, *An unexpected correlation between cardinal temperatures of microbial growth highlighted by a new model*, *J. Theor. Biol.*, 1993, 162(4), 447–463.
- [27] J. M. Smith, *Evolution and the Theory of Games*, 1982.
- [28] M. Striebel, S. Schabhuttel, D. Hodapp et al., *Phytoplankton responses to temperature increases are constrained by abiotic conditions and community composition*, *Oecologia*, 2016, 182(3), 815–827.
- [29] M. K. Thomas, C. T. Kremer and C. A. Klausmeier, *A global pattern of thermal adaptation in marine phytoplankton*, *Science*, 2012, 338(6110), 1085–1088.
- [30] J. Uitz, H. Claustre, A. Morel et al., *Vertical distribution of phytoplankton communities in open ocean: An assessment based on surface chlorophyll*, *J. Geophys. Res. Oceans*, 2006, 111, 8.
- [31] X. Wang, M. Fan and L. Hao, *Adaptive evolution of foraging-related trait in intraguild predation system*, *Math. Biosci.*, 2016, 274, 1–11.
- [32] J. Zu, M. Mimura and W. J. Yuichiro, *The evolution of phenotypic traits in a predator-prey system subject to Allee effect*, *J. Theor. Biol.*, 2010, 262(3), 528–543.
- [33] J. Zu and T. Yasuhiro, *Adaptive evolution of anti-predator ability promotes the diversity of prey species: Critical function analysis*, *BioSystems*, 2012, 109(2), 192–202.